34th Annual International Conference of the IEEE EMBS
San Diego, California USA, 28 August - 1 September, 2012

High Precision Semi-Automated Vertebral Height Measurement Using Computed Tomography: a Phantom Study

Sovira Tan, Jianhua Yao, Lawrence Yao, and Michael M. Ward

Abstract—**The measurement of vertebral heights is necessary for the evaluation of many disorders affecting the spine. High precision is particularly important for longitudinal studies where subtle changes are to be detected. Computed tomography (CT) is the modality of choice for high precision studies. Radiography and dual emission X-ray absorptiometry (DXA) use 2D images to assess 3D structures, which can result in poor visualization due to the superimposition of extraneous anatomical objects on the same 2D space. We present a semi-automated computer algorithm to measure vertebral heights in the 3D space of a CT scan. The algorithm segments the vertebral bodies, extracts their end plates and computes vertebral heights as the mean distance between end plates. We evaluated the precision of our algorithm using repeat scans of an anthropomorphic vertebral phantom. Our method has high precision, with a coefficient of variation of only 0.197% and Bland-Altmann 95% limits of agreement of [-0.11, 0.13] mm. For local heights (anterior, middle, posterior) the algorithm was up to 4.2 times more precise than a manual mid-sagittal plane method.**

I. Introduction

RELIABLE measurement of vertebral height may benefit many clinical and research applications. Vertebral height is measured to assess the outcome of restoration procedures [1] and to optimize the fit of implants and prostheses [2]. Vertebral height measurement has been crucial in the study of osteoporosis. Osteoporosis is a progressive skeletal disease characterized by low bone mass leading to fractures in the spine, hip, and wrist. Vertebral compression fracture, which results in the loss of vertebral height, can be used to monitor the progress of the disease. Clinical trials of osteoporosis medications typically assess their efficacy in halting bone fracture by estimating changes in vertebral heights over a period of a few years. The current standard method involves the semi-quantitative scoring or morphometric measurement of vertebral bodies on radiographs [3, 4] or DXA [5, 6]. The precision of the methods may be compromised by the limitations of the modalities: 1) use of 2D images to assess 3D structures arrayed in space, 2) poor visualization due to the superimposition of extraneous anatomical objects on the same 2D space. A more precise method is desirable because smaller samples would be needed to detect statistically significant differences. Trial duration could also be shortened.

To improve precision, we present a semi-automated computer algorithm that quantitatively measures vertebral heights in CT scans. The method utilizes the complete 3D information that CT scans provide about anatomical structures. CT can achieve better resolution than magnetic resonance imaging (MRI). CT also provides a better visualization of bone than MRI. Moreover our algorithm reduces intra- and inter-reader variability through automation. Automation is also essential as manual measurement of vertebral height on every slice of a CT scan could be prohibitively labor-intensive and time-consuming. Previously reported methods using CT only take measurements on the mid-sagittal slice [2, 7].

A precision study quantifies the variability associated with repeat measurements, which is crucial for determining what can reliably be considered true change. We present a precision study of our approach using repeat CT scans of an anthropomorphic spine phantom. This allowed us to evaluate the variability associated with the imaging modality, its limitations, distortions and artifacts. As these often depend on the position of the subject relative to the imaging system, the phantom was moved between scans.

II. Materials and Methods

A. Spine phantom and scanning protocol

The vertebral phantom was manufactured by CIRS (Norfolk, VA). It consists of 5 anthropomorphic vertebral bodies, which had cortical and trabecular bone made of epoxy resin of different densities (respectively 1200mg/cc in a soft tissue matrix and 250mg/cc of calcium hydroxyapatite in a marrow equivalent matrix). The phantom is contained in an acrylic tank. The tank was filled with water to provide an interface with the epoxy resin similar to the interface between cortical bone and soft tissue in vivo.

The phantom was scanned 12 times on Philips Brilliance 64 and 12 times on a GE Lightspeed Ultra. The former is 64-detector row scanner while the latter is an older 8-detector row scanner. For both scanners, voltage and current parameters were 120 kVp, 300 mAs respectively. Slice thickness was 1.5 and 1.25 mm respectively for the Philips and GE. For each scan, three reconstructions were made at field of view (FOV) diameters 25, 40 and 48 cm

This research was supported by the Intramural Research Program of the NIH, NIAMS and CC.

S. Tan and M. M. Ward are with the National Institute of Arthritis and Musculoskeletal and Skin diseases, National Institutes of Health, Clinical Center, 10 Center Drive MSC 1182, Bethesda, MD 20892 USA (e-mail: tanso@ mail.nih.gov).

J. Yao, and L. Yao are with the Department of Diagnostic Radiology, National Institutes of Health, Clinical Center, Bethesda, MD 20892 USA.

corresponding to axial in-plane pixel sizes of about 0.49, 0.78 and 0.94 mm, which we respectively call high, medium and low resolutions. The phantom was slightly rotated on the scanner table after each scan.

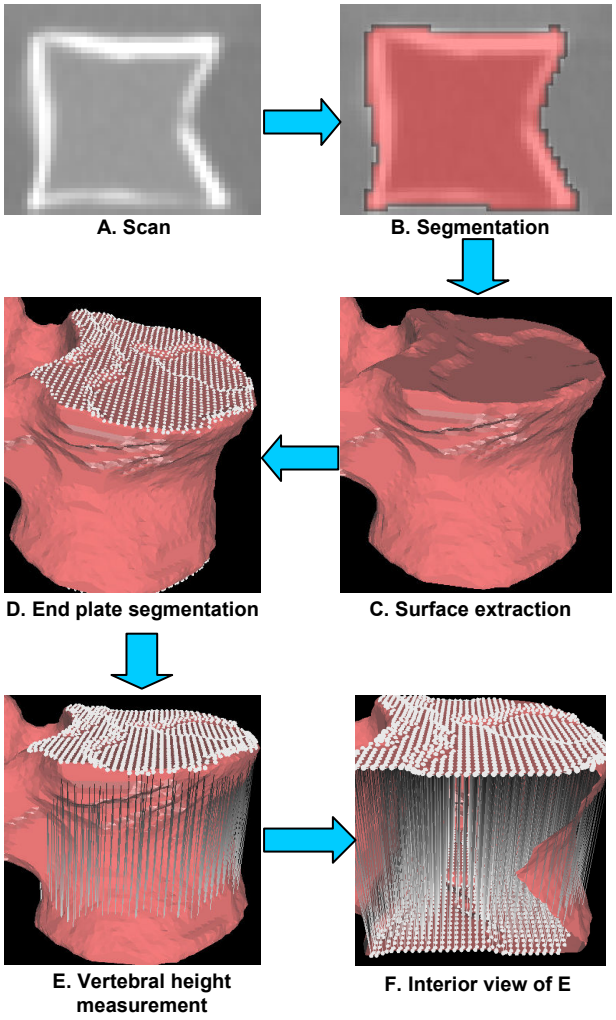

Fig. 1. Overview of the algorithm. In F, a portion of the mesh in E was removed to show measurements in the interior of the vertebral body.

B. Computer aided vertebral height measurement

Our algorithm for vertebral height estimation is summarized in Fig. 1. Fig. 1-(A) shows a sagittal slice of the scanned phantom. From user provided seeds, the vertebral bodies are segmented using a method based on level sets (Fig. 1-(B)). Triangular meshes representing the surfaces of the segmentations are then extracted using the Marching Cubes algorithm (Fig. 1-(C)) [8]. The end plates of the vertebral bodies are then segmented using a level set evolving on the triangular meshes (Fig. 1-(D)). Finally, vertebral heights are computed as the mean distances between opposite end plates of vertebral bodies (Fig. 1-(E)-(F)). The vertices of the meshes naturally sample the surfaces uniformly and densely. For each vertex on the upper end plate we find the vertex on the lower end plate that is most aligned with the normal direction of the end plates. Each pair of vertices thus formed constitutes a sample measurement of vertebral height. Such sample measurements are represented by gray segments in Fig. 1-(E)-(F). Those individual measurements are then averaged to yield an estimate of the vertebral height.

Segmentation: Both the vertebral body and end plate segmentation are performed using the level set method. Level sets are evolving contours that can expand, contract and even split or merge [9]. They can be designed to deform so as to match an object of interest and stop at its boundaries. A widely used level set, the geodesic active contour (GAC), can be written [10]:

$$\frac{d\psi}{dt} = \alpha g c |\nabla \psi| + \beta g \kappa |\nabla \psi| + \gamma \nabla g \nabla \psi \qquad (1)$$

The evolving contour is encoded as the zero level set of the distance function $\psi(\vec{x},t)$. In other words, points that verify $\psi(\vec{x},t)=0$ form the contour. By convention, the distance is negative for points inside the contour and positive for the ones outside:

$$\psi(\vec{x},t) = \pm d \qquad (2)$$

where d is the distance from point $\vec{x}$ to the zero level set contour. The first term on the right-hand side of the Equation 1 is the propagation term that makes the contour move with velocity c. The second term, the curvature term, controls the smoothness of the contour using the mean curvature κ. The third term, the advection term, locks the contour to the boundary. The parameters α, β and γ weight the importance of each term.

The spatial function g, contains information about the objects' boundaries and is often called the speed function. The speed function guides the level set. It should ideally have values close to 1 where there are no boundaries (so that the level set can expand rapidly) and values close to 0 where boundaries are present (so that the level set stops).

Level set are usually implemented in the Cartesian domain of rectangular grids, but they can also be written for the domain of a surface mesh [11]. However, the boundary information that needs to be encoded in the speed function is very different in the 2 cases. For a Cartesian grid (Fig. 1-(A)), boundaries are usually defined by grey level gradients. In our case, the level set starts roughly in the middle of the vertebral body where grey level gradients are low and stops at the cortical bone where grey level gradients are high. However, for a triangular mesh representing a 3D surface (Fig. 1-(C)), the relevant feature is curvature. In our case, the level set starts roughly in the middle of the end plate which is flat (low curvature) and stops at the ridgeline where curvature is high. A detailed account of both the vertebral body and end plate segmentation can be found in [11].

Vertebral height measurement: Height is measured along the direction defined by the normal, $\vec{N}$, to the 2 end plates of each vertebral body. A least square method is used to fit a plane to both end plates [11]. We take the average of those 2 normals as an estimate of $\vec{N}$. For each vertex on the upper end plate we find its counterpart on the lower end plate, that is, the vertex on the lower end plate that is most aligned along the direction of $\vec{N}$. Let U be a vertex of the upper plate. Its counterpart L on the lower end plate is defined as the vertex that maximizes the scalar product:

$$S = \overrightarrow{UL} \cdot \vec{N} \qquad (3)$$

All vectors being normalized to a unit length, $\overrightarrow{UL}$ and $\vec{N}$ are perfectly aligned when S is equal to 1. Any deviation results in a lower scalar product.

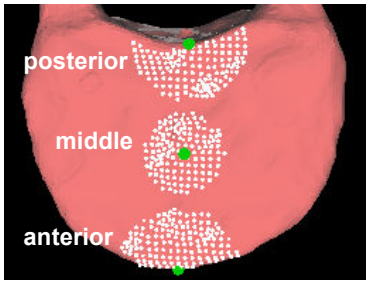

Fig. 2. Anterior, middle and posterior areas for local height measure. The green points represent the anterior, middle and posterior points.

The distance between every pair of corresponding vertices provides a local measure of vertebral height. To estimate the global vertebral height, we average all the distances (Fig. 1-(E)-(F)). However, height can also be estimated for local areas of the end plate. In particular, for the evaluation of vertebral fractures, it is desirable to estimate vertebral height locally at anterior, middle and posterior positions. This allows the identification of different types of fracture: wedge, biconcave and crush [3]. Fig. 2 shows the 3 areas (anterior, middle and posterior) within which we can restrict height computation. These local areas are defined in the following manner. We first determine the middle, anterior and posterior points (green in Fig. 2). The middle point is computed as the average of all end plate points. The anterior and posterior points are the end plate points along the y-axis (sagittal direction) furthest from the central point. The anterior, middle and posterior areas are then defined as the sets of points closest to the anterior, middle and posterior points, respectively. We evaluated the precision of the algorithm when the size of each of the local areas is limited to 15% of the end plate surface.

To compare the precision of the automated algorithm to that of a manual method, we measured local heights manually on the mid-sagittal slice of the CT scans using the Carestream PACS software (Carestream, Rochester, NY). One operator carried out the measurements on the 6 pairs of high resolution reconstructions from the 64-detector row scanner. Fig. 3 shows one pair of measurements for one of the phantom's vertebral bodies.

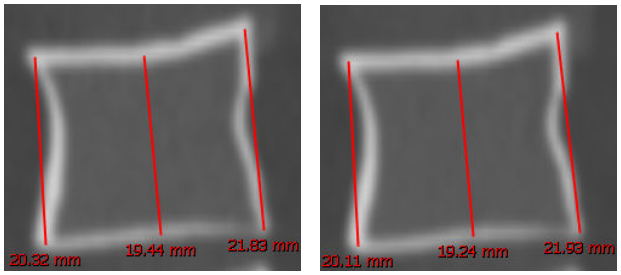

Fig. 3. Mid-sagittal plane manual measurement of local vertebral heights on a pair of vertebral bodies.

Statistical analysis: We analyzed the differences in absolute value between computed inter-scan height measures. The mean and standard deviation of the differences constitute our measure of precision. Smaller differences indicate better precision. We used Bland-Altman analysis evaluate the 95% agreement limits. Coefficients of variation (CV) were also evaluated.

III. Experimental Results

A. 64-detector row versus 8-detector row

To investigate the impact of technological advances, we stratified the measurement differences into 2 categories corresponding to the 2 scanners (64- and 8-detector row). The 12 scans for each scanner are coupled randomly into 6 pairs. For each scan, 3 reconstructions at 3 resolutions are available. For this first experiment, all resolutions were used. For each scanner, the total number of vertebral height measurement differences is therefore n=5x6x3=90. The results (Table I) show that the 64-detector row scanner has excellent precision with a CV of only 0.239%. Comparing the CVs of the 2 scanners, it was observed that the 64-detector row was about 3 times more precise than the 8-detector scanner. As 8-detector row scanners are now being phased out, the results obtained with the 64-detector row scanner are the most relevant. In the rest of the paper we will only report the results of the 64-detector row scanner.

TABLE I
PRECISION OF VERTEBRAL HEIGHT MEASUREMENTS FOR THE 64- AND 8-DETECTOR ROW SCANNER

Inter-scan differences	8-detector row	64-detector row
mean (mm)	0.17	0.056
SD (mm)	0.13	0.047
CV (%)	0.683	0.239
95% limits of agreement (mm)	-0.42, 0.41	-0.13, 0.15

B. The influence of image resolution

To investigate the influence of the 3 image resolutions we stratified the results into the corresponding 3 groups. The total number of vertebral height measurement differences for each resolution is n=5x6=30. The CV results (Table II) show that high resolution reconstructions yield marginally better precision than medium resolution. The gain in precision of both high and medium over low resolution is more substantial.

TABLE II
PRECISION OF VERTEBRAL HEIGHT MEASUREMENTS FOR HIGH, MEDIUM AND LOW RESOLUTIONS

Inter-scan differences	High	Medium	Low
mean (mm)	0.048	0.045	0.074
SD (mm)	0.036	0.042	0.056
CV (%)	0.197	0.203	0.301
95% limits of agreement (mm)	-0.11, 0.13	-0.11, 0.13	-0.17, 0.19

C. Local height, automated versus manual measurement

This study was restricted to the high resolution reconstructions. In addition to the anterior, middle and posterior heights, we also computed the anterior-posterior ratio (AP) and the middle-posterior ratio (MP) [3]. For each of the local heights and the ratios, the total number of measurement differences is n=5x6=30.

The CVs in Table III indicate that for the anterior, middle and posterior heights, the automated method is respectively 4.2, 3.2 and 3.1 times more precise than the mid-sagittal manual measurement. For the AP and MP ratios respectively, the automated method is 3.3 and 3.7 times more precise.

TABLE III
PRECISION OF LOCAL VERTEBRAL HEIGHT MEASUREMENTS FOR THE AUTOMATED AND MANUAL METHODS

	Inter-scan differences	mean (mm)	SD (mm)	CV (%)
AUTOMATED	Anterior	0.065	0.052	0.275
	Middle	0.049	0.063	0.271
	Posterior	0.073	0.067	0.317
	AP ratio	0.0044	0.0028	0.377
	MP ratio	0.0027	0.0021	0.257
MANUAL	Anterior	0.25	0.19	1.14
	Middle	0.20	0.13	0.875
	Posterior	0.24	0.16	0.982
	AP ratio	0.014	0.010	1.26
	MP ratio	0.0093	0.0077	0.945

IV. Conclusion

We have presented a novel semi-automated algorithm for measuring vertebral heights in the 3D space of CT scans. The method is designed for applications that require high precision. We evaluated the precision of our algorithm using an anthropomorphic vertebral phantom. Repeat scans and repositioning of the phantom allowed us to investigate the variability associated with the distortions and artifacts of the imaging modality.

Our results suggest that 64-detector row scanner technology is more precise than 8-detector row scanner technology and that precision improves with resolution The best results obtained (high resolution and 64-detector row scanner) indicate that the method is highly precise, with a coefficient of variation of only 0.197% and Bland-Altmann 95% limits of agreement of [-0.11, 0.13] mm. For local heights (anterior, middle, posterior) the algorithm was up to 4.2 times more precise than a manual mid-sagittal plane method.

References

[1] G. Sun, P. Jin, M. Li, X. W. Liu, and F. D. Li, "Height restoration and wedge angle correction effects of percutaneous vertebroplasty: association with intraosseous clefts.," *Eur Radiol,* vol. 21, pp. 2597-603, Dec 2011.

[2] S. H. Zhou, I. D. McCarthy, A. H. McGregor, R. R. Coombs, and S. P. Hughes, "Geometrical dimensions of the lower lumbar vertebrae--analysis of data from digitised CT images.," *Eur Spine J,* vol. 9, pp. 242-8, Jun 2000.

[3] H. K. Genant, C. Y. Wu, C. van Kuijk, and M. C. Nevitt, "Vertebral fracture assessment using a semiquantitative technique.," *J Bone Miner Res,* vol. 8, pp. 1137-48, Sep 1993.

[4] G. Guglielmi, D. Diacinti, C. van Kuijk, F. Aparisi, C. Krestan, J. E. Adams, and T. M. Link, "Vertebral morphometry: current methods and recent advances.," *Eur Radiol,* vol. 18, pp. 1484-96, Jul 2008.

[5] G. M. Blake, J. A. Rea, and I. Fogelman, "Vertebral morphometry studies using dual-energy x-ray absorptiometry.," *Semin Nucl Med,* vol. 27, pp. 276-90, Jul 1997.

[6] M. G. Roberts, E. M. Pacheco, R. Mohankumar, T. F. Cootes, and J. E. Adams, "Detection of vertebral fractures in DXA VFA images using statistical models of appearance and a semi-automatic segmentation.," *Osteoporos Int,* vol. 21, pp. 2037-46, Dec 2010.

[7] S. Ghosh, R. S. Alomari, V. Chaudhary, and G. Dhillon, "Automatic Lumbar Vertebra Segmentation from clinical CT for Wedge Compression Fracture Diagnosis," *Proceedings of SPIE Medical Imaging,* vol. 7963, p. 796303, 2011.

[8] W. E. Lorensen and H. E. Cline, "Marching cubes: a high resolution 3D surface construction algorithm," *ACM SIGGRAPH Computer Graphics,* vol. 21, pp. 163-169, 1987.

[9] J. A. Sethian, *Level set methods and fast marching methods: evolving interfaces in computational geometry, fluid mechanics, computer vision and materials science*: Cambridge University Press, 1999.

[10] V. Caselles, R. Kimmel, and G. Sapiro, "Geodesic active contours," *International Journal of Computer Vision,* vol. 22, pp. 61-79, FEB-MAR 1997.

[11] S. Tan, J. Yao, M. M. Ward, L. Yao, and R. M. Summers, "Computer aided evaluation of ankylosing spondylitis using high-resolution CT.," *IEEE Trans Med Imaging,* vol. 27, pp. 1252-67, Sep 2008.